A Novel Granulation Technology for Producing Spherical Wax Particles

By *Jiu-Yang Fang*, *Yuan-Zhou Xi*, *Ting-Jie Wang**, and *Yong Jin*

A novel granulation technology for producing spherical wax particles that makes use of the insolubility of wax and water is developed. The granulation is stably performed in a granulator with a water-cooling tower. The granulation process is analyzed and the influences of key factors on the process are studied. Experiments are carried out with 58# semi-refined wax and 70# crystallitic wax in an experimental granulator which has 118 nozzles (D_i = 0.96 mm, D_o = 1.28 mm). The process capacity and the corresponding particle diameter are 55–60 kg/h and 4–5 mm, respectively. Using the modified correlation of Scheele and Meister, suitable operation flow rates and the corresponding particle diameters for different nozzles can be predicted. This technology has the following advantages: good particle shape with excellent fluidity, high process capacity and heat-transfer efficiency, and a small space for the granulator. It is also suitable for producing spherical particles of other materials, which have similar physical properties to wax.

1 Introduction

Wax is an important product in oil refineries, especially when the feed is wax-based crude oil. Some wax-based crude oil can contain about 45 % wax, e.g., the crude oil from Northern Shenyang in China [1,2]. Wax is widely used in many fields, such as rubber, textile, medicine, telecommunication materials, wood manufacture, food production, foundry, etc. Generally, there are two ways of wax transportation from the refinery to the consumer. One is by transporting the solidified wax, and the other is by transporting melted wax using good temperature insulation, and the latter is only suitable for large consumers. Devices for preserving and transporting melted wax are very complex and have high energy consumption. The molding of melted wax is an important process in wax production.

Presently, there are three major wax molding technologies. One is wax-slab molding with a chain-tray system. One is wax-flake molding with a belt cooler. The third is wax-powder molding. In the first technology, the melted wax is filled into trays of a definite volume, and the trays are sent into a cooling room by a chain driver. Wax is solidified into wax slabs and removed from the trays after about 2 hours cooling in the cooling room. Since cooling air is used as the medium of heat transfer, this molding process has low heat transfer efficiency, a huge device, a complicated mechanical structure and a high failure rate. Each wax slab usually weighs 5 kg. Many customers have to crush the wax slabs before using or re-melting them. Thus, it is not convenient to use wax slabs, especially for customers who consume a small amount of wax. In the second technology, melted wax is dropped onto a moving belt from a drum, cooling water is sprayed onto the back surface of the stainless steel belt, and solidified wax flakes are scraped off from the belt by a scraper. Since the thermal conductivity of wax is only about 0.2 W/m·K and heat transfer from the wax to the water is indirect via the belt, the necessary length of the belt is usually over 30 meters. The molding equipment has a very complicated structure and a relatively high failure rate. In the third technology, melted wax is sprayed into an air cooling tower, wax droplets are solidified into 0.1–0.2 mm pellets. Since the convective heat-transfer coefficient of air is low, the air cooling tower usually has a height of 15–25 m to ensure the solidification of wax pellets.

Spherical wax particles have a good shape and excellent flowability, and are easy to quantify, pack and transport. In addition, with spherical wax particles, no crushing is needed before use or remelting. These characteristics are desired by both producers and consumers. In order to overcome the deficiencies of present wax molding techniques, a new technology for wax granulation in a water-cooling tower is developed that makes use of the insolubility of wax and water. The granulation principle, process and operation parameters are given in this paper. The key factors in the granulation process are analyzed. 58# semi-refined wax and 70# crystallitic wax (melting points in the range of 58–60 °C and 70–72 °C, respectively) are used in an experimental granulator with 118 nozzles (D_i = 0.96 mm, D_o = 1.28 mm) at a capacity of 55–60 kg/h and spherical wax particles of 4–5 mm are obtained.

2 Granulation Design

2.1 Overall Granulation Flow

The overall granulation flow diagram is shown in Fig. 1. Melted wax from the nozzles forms drops in the granulation hole where there is a local region near the nozzle that is at a high temperature. Since the densities of the wax drop and particles are lower than water, the wax drops rise through the granulation hole and into the tower kept at a low temperature, where the wax drops are cooled into spherical par-

[*] Jiu-Yang Fang, Yuan-Zhou Xi, Ting-Jie Wang (e-mail: wangtj@mail.tsinghua.edu.cn), Yong Jin, Department of Chemical Engineering, Tsinghua University, Beijing 100084, China.

 DOI: 10.1002/ceat.200402036

ticles. At the top of the tower the particles are discharged by the circulatory overflow. The particles are separated from the overflow water and re-cooled by spraying cool water so that the particles are fully cooled. Subsequently, the particles are dehydrated in a vibratory screen, where most of the surface water on the wax particles is removed. After that, the particles are air-dried in a fluidized bed, and good spherical wax particles are obtained.

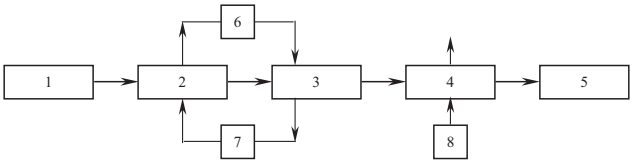

Figure 1. Granulation flow diagram; 1. wax feed; 2. granulator; 3. vibratory screen; 4. air dryer; 5. product; 6. cooler; 7. pump; 8. fluidization air.

The overflow water and the cooling water used for spraying flow into a buffer tanker for recycle. Part of the water from the tanker is refrigerated as cooling water, and the rest is used as circulatory overflow. The vibratory screen is operated at a high vibration frequency and low amplitude to increase its effectiveness in removing free water on the particle surface and to avoid serious friction between particles. After dehydration by the vibratory screen, the free water content on the particle surface is usually below 2 %. As the wax is hydrophobic, the water on the particle surface can easily be removed in a fluidized bed using air at a certain temperature.

2.2 Structure of the Granulator

The structure of the granulator is shown in Fig. 2. The experimental granulator is 300 mm in length, 200 mm in width, and 1400 mm in height. The melted wax is fed into the wax chamber by a pump operating at a fixed flow rate. The combined distributor, which includes a switch board and a heating board, is placed above the wax chamber. The switch board controls the switching on and off of the melted wax flow through the nozzles. The heating board above the switch board is used to heat the water in the granulation hole to form a local region of high temperature, to ensure spherical drop formation from the nozzles by the action of interfacial tension.

The structure of the distributor in the experiments is shown in Fig. 3. The thickness of both the heating board and that of the switch board are 20 mm. The switch board and heating board are made of aluminum, which has excellent thermal conductivity. Both sides of the two boards are coated with a heat insulating layer to prevent heat transfer from the heating boards to the cool water above and from the switch board to the melted wax below. The granulation holes are drilled vertically in the heating board. The diameter of the granulation holes is 12 mm. Horizontal holes called heating holes are drilled in the heating board from the side wall.

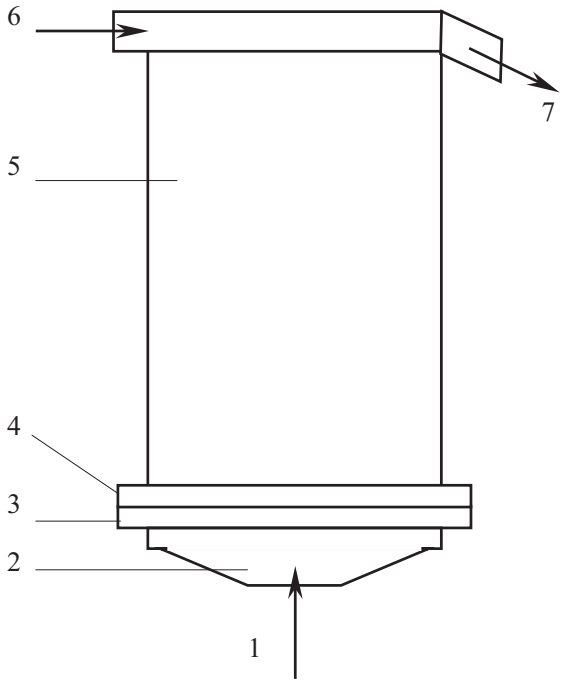

Figure 2. The granulator structure; 1. wax feed; 2. wax chamber; 3. switch board; 4. heating board; 5. cooling tower; 6. in-let of water; 7. out-let of water.

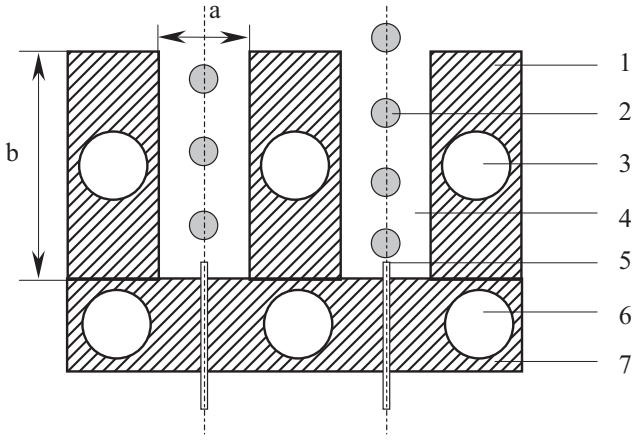

Figure 3. The structure of combined distributor; 1. heating board; 2. wax drop; 3. heating hole; 4. granulation hole; 5. nozzle; 6. heating/cooling hole; 7. switch board; a = 12 mm; b = 20 mm.

Water in the granulation holes is heated by a heating medium flow in the heating holes, which maintains a constant temperature inside. A group of nozzles are fixed in the switch board, which is under the heating board. Each nozzle corresponds one-to-one to the center of a granulation hole. Horizontal holes are also drilled in the switch board from the side wall. Heating medium or cooling medium can be switched into the horizontal holes in the switch board to switch on or off the granulation. When the cooling medium is switched to enter the horizontal holes, the switch board is cooled and the melted wax in the nozzles is solidified, thus the "switch off" function of the granulation is executed. When the heating medium is switched to enter the horizon-

tal holes, the switch board is heated and the solidified wax in the nozzles is melted, thus the "switch on" function of the granulation is executed. Hot water and cool water are used as the heating medium and cooling medium respectively in the experiments.

3 Drop Formation and Solidification

3.1 Drop Formation

Melted wax is injected from the nozzle and forms a series of drops. Drop formation at the tip of the nozzle can be regarded as occurring in two stages: a static drop stage when only the inflation of the drop takes place and a necking stage when the drop rises, necks and gets detached from the nozzle [3,4]. In the two stages, the main forces acting on the drop are buoyancy, inertial, interfacial tension and drag forces. When the four forces at equilibrium[1]:

$$F_B + F_I = F_S + F_D \tag{1}$$

The drop volume from the above equations is:

$$V_{ES} = \frac{\pi\sigma D_N}{g\Delta\rho} + \frac{20\mu_c Q D_N}{D_E^2 g\Delta\rho} - \frac{4\rho_d Q u_N}{3g\Delta\rho} \tag{2}$$

During the necking process, a considerable amount of liquid flows into the drop after the net lifting forces exceed the net restraining forces, and contributes to the final drop volume. The additional volume V_{EN} during drop necking can be calculated from the equation:

$$V_{EN} = 4.5\left(\frac{Q^2 D_N^2 \rho_d \sigma}{(g\Delta\rho)^2}\right)^{1/3} \tag{3}$$

Combining Eq. (2) and Eq. (3), and considering the drop volume loss due to the liquid which remains at the tip of the nozzle after the drop breaks off, the final drop volume can be expressed with a correction factor as follows:

$$V_E = F\left[\frac{\pi\sigma D_N}{g\Delta\rho} + \frac{20\mu_c Q D_N}{D_E^2 g\Delta\rho} - \frac{4\rho_d Q u_N}{3g\Delta\rho} + 4.5\left(\frac{Q^2 D_N^2 \rho_d \sigma}{(g\Delta\rho)^2}\right)^{1/3}\right] \tag{4}$$

where D_N is the inner diameter of the nozzle, cm; g is the gravitational constant, 980 cm/s^2; Q is the volumetric flow rate of the dispersed phase (wax), cm^3/s; u_N is the average velocity of the dispersion phase through the nozzle, cm/s; V_E is the drop volume after break off from the nozzle, cm^3; D_E is the diameter of the detached drop, cm; μ_c is the viscosity of the continuous phase (water), g/(cm·s); ρ_c, ρ_d are the densities of the continuous and dispersed phases, g/cm^3; σ is the interfacial tension, dyne/cm; F is the Harkins-Brown correction factor for the part of the liquid that remains on the nozzle tip after the detachment of the drop [5]. Horvath *et al.* [6] derived an approximate equation for the estimation of F values:

$$F = 0.6 + 0.4\exp\left\{-2D_N\left(\frac{g\Delta\rho}{\pi\sigma D_N}\right)^{1/3}\right\} \tag{5}$$

The drop volume of the melted wax formed at the nozzle tip can be calculated by Eq. (4).

3.2 Drop Solidification

The water in the granulation hole is kept at a fixed temperature above the melting point of the wax by controlling the flow rate of the heating medium in the horizontal holes in the heating board. This enables spherical drop formation in the granulation holes. These drops rise into the low temperature region in the tower and solidify into particles there. During the rise, the wax drops change in phase from liquid to solid, and their average temperature decreases gradually. The surface of the wax drop first solidifies, and the solid-liquid interface of the wax contracts toward the drop center until the whole drop solidifies. However, since wax is a mixture of a variety of hydrocarbons, the phase change occurs over a temperature range instead of at one temperature. The solidification of a wax drop can be approximately expressed by the following equations:

In the solid region:

$$\frac{\partial T_s}{\partial t} = \alpha_s \nabla^2 T_s \tag{6}$$

In the liquid region:

$$\frac{\partial T_l}{\partial t} = \alpha_l \nabla^2 T_l \tag{7}$$

At the solid-liquid interface:

$$k_s\left(\frac{\partial T_s}{\partial n}\right)_\xi - k_l\left(\frac{\partial T_l}{\partial n}\right)_\xi = \lambda\rho v_\xi \tag{8}$$

and

$$v_\xi = \frac{d\xi}{dt} \tag{9}$$

Where l, s and ξ denote the liquid phase, solid phase and solid-liquid interface, respectively; T is the temperature, °C; t is time, s; α is thermal diffusivity, m^2/s; k is thermal conductivity, W/(m·K); λ is the latent heat of phase change, J/kg; v_ξ is the moving velocity of the solid-liquid interface, m/s.

The average convective heat transfer coefficient between particle and water can be calculated with the rise velocity and the particle size. With the use of perturbation method [7,8], an approximate solution of the heat transfer process

1) List of symbols at the end of the paper.

and the necessary cooling time can be calculated. By analyzing the moving velocity of the phase interface, the minimum residence time for the drop to be cool enough so that the wax particles do not stick to each other can be obtained.

To get the minimum residence time for drops of 4–5 mm in the cooling tower, it is assumed that the wax particles do not stick to each other when 60 % volume of the wax drop solidifies inward. In case of melted 58# semi-refined wax at 70 °C and a water temperature from 40 °C to 45 °C, the calculated cooling time is 7–8 seconds. For melted 70# crystallitic wax at 90 °C and water temperature from 49 °C to 58 °C, the calculated cooling time is 6–7 seconds.

Experimental results are reasonably consistent with the calculated value. 7–8 seconds for cooling of 58# semi-refined wax and 6–7 seconds for cooling of 70# crystallitic wax can form a solid crust of definite thickness to ensure stable granulation.

4 Key Factors in Wax Granulation

The widely used 58# semi-refined wax and 70# crystallitic wax are taken as feeds in the experiments. The properties relevant to the granulation process of the two kinds of wax are listed in Table 1.

The temperature of melted wax affects granulation stability to a certain extent. Experiments show that the suitable temperature for the feed wax is 10–15 °C higher than the melting temperature of the wax, which is close to the temperature of the wax product from the refinery.

4.1 The Drop Formation Process

4.1.1 Flow Rate of the Melted Wax in the Nozzle

The flow rate of the melted wax in the nozzle affects the drop formation. When the flow rate is in a relatively low range, a series of drops of a uniform size form in a single file. When the flow rate increases, the drop formation frequency increases and the drop volume increases slightly. When the flow rate exceeds a critical value called the jetting rate, jet flow happens and a lot of small drops with a wider size distribution form. The granulation holes may be jammed and the drops are easily agglomerated in the tower, leading to unstable granulation.

The granulation in this research is performed at a relatively low flow rate of melted wax. The drop size depends on the wax flow rate in the nozzle, the nozzle structure (such as inner diameter and wall thickness), the interfacial tension between the melted wax and water, etc. In a stable granulation, there is a weak dependence of the wax flow rate on the drop size. This shows that the granulation process can be stably operated in a relatively wide range of the flow rate.

4.1.2 Temperature in the Granulation Hole

The melted wax breaks off from the nozzle and spherical drops form in the granulation hole. The temperature in the granulation hole should be higher than the wax melting point for stable drop formation. The water in the granulation hole is heated by the heating board and kept at a constant temperature in order to satisfy the temperature requirement for stable drop formation. The upper surface of the heating board is coated with a thermal insulating layer to prevent heat transfer from the board to the water above it. The temperature in the granulation hole fluctuates within a certain range due to drop movement and natural convection. The experiments show that the temperature in the hole should be 5–8 °C above the melting point of the wax for stable granulation.

4.1.3 Temperature of the Switch Board

The main function of the switch board is to start or shut down the granulation process. The nozzles are kept sealed with wax before the granulation, cooling medium is fed through the horizontal holes of the switch board, and the temperature of the switch board can be controlled at 20 °C below the melting point of the wax. The water in the granulation hole above the switch board is prevented from flowing into the wax chamber below. When granulation begins, the heating medium is switched to flow into the horizontal holes. The temperature of the switch board is increased and controlled at about 20 °C above the melting point of the wax. The solidified wax in the nozzle is melted within 10 seconds, and drops form through the nozzle. When granulation needs to be shut down, the cooling medium is switched into the horizontal holes instead of the heating medium, the wax in the nozzle is solidified in a few seconds and the nozzles are blocked, and drop formation stops.

Table 1. Basic physical properties of 58# semi-refined wax and 70# crystallitic wax.

Wax	Melting point, °C	Density (solid), kg/m^3	Density (liquid), kg/m^3	Interfacial tension (wax-water), mN·m^{-1}	Viscosity, cp
58# (White)	58–60	898.2 (20 °C)	782.3 (70 °C)	18.40 (70 °C)	6.26 (70 °C)
70# (Yellow)	70–72	896.2 (20 °C)	772.7 (80 °C)	17.54 (80 °C)	8.73 (80 °C)

4.2 The Drop Solidification Process

4.2.1 Temperature Distribution in the Tower

After a drop forms in the granulation hole, it rises in the tower and is cooled during the rising process. A suitable temperature distribution in the tower should be maintained to cool and solidify the drop. If the temperature in the tower is kept relatively low, heat transfer from the heating board to the water above the board in the tower increases, resulting in the increase of energy consumption. Therefore, a distribution of temperature decreasing from the bottom to top in the tower is desirable for decreasing energy consumption.

The temperature of the water in the upper tower is kept relatively low by the circulatory overflow on the top of the tower. A gradually decreasing temperature distribution from the bottom to the top in the tower forms due to the heat transfer of water convection, heat transfer from the wax particles to the water, and the particle movement. The wax particles are discharged by the circulatory overflow at the top of the tower. Since the thermal conductivity of the wax is quite low, the particles can be completely cooled only if the temperature in the tower is low enough or the tower is high enough. Both options are not optimal for the design. Therefore, a two-stage cooling of the particles is designed in the drop solidification process. The first stage is for the particles to be preliminarily cooled in the tower, when they form a solid shell that prevents them from sticking to each other. After the particles are overflowed from the tower, most of the water is separated from the particles and a second stage of cooling is performed by spraying cooling water on the particles. Hence, the height of the tower can be reduced and the cooling efficiency is increased. The temperature and the flow rate of the circulatory water directly affect the temperature distribution in the tower. In order to remove the particles on the top of the tower, the water height of the overflow should be kept about 10 mm or a little higher. The inlet and outlet weirs for the circulatory water are designed flatly and sleekly. The circulatory water is distributed uniformly along the inlet width and overflows smoothly into the tower. The inlet and outlet structures of the circulatory water are so designed that the overflow water flows smoothly at the top of the tower. By doing so, the disturbance of the water in the cooling tower can be reduced, which helps to maintain the desirable temperature distribution in the whole tower.

Fig. 4a shows that the temperature distribution in the tower of stable granulation for 58# semi-refined wax in three experiments. The position of 0 in the horizontal axis is the upper surface of the heating board. The first point corresponds to the average temperature in the granulation hole. Fig. 4a shows that the average temperature in the granulation hole is about 70 °C, the temperature in the tower is in the range 40–43 °C, and the temperature at the top of the tower is relatively low because of the circulatory overflow. The temperature difference between the water in the granulation hole and the water in the tower reaches about 30 °C. This enables the spherical drops to form in the granulation hole and to be solidified in the tower where the temperature is relatively low. In this way energy consumption is saved.

The experiments show that when the average temperature in the tower is in the range 40–43 °C and the residence time of the particles in the tower is about 8 seconds, the surface layer of the wax particles can be cooled sufficiently that wax particles do not stick to each other. The particles from the circulatory overflow can be fully cooled after spraying with cool water at about 20 °C. If the temperature in the tower is too high, particles cannot be adequately cooled in the tower and tend to stick to each other. If the temperature in the tower is too low, the water temperature difference between the inside and outside of the granulation hole becomes large and heat convection is intensified. In this case, it is difficult to maintain the temperature of the hole and energy consumption increases.

Similarly to 58# semi-refined wax, the temperature distribution of stable granulation in the tower for 70# crystallitic wax in experiments is shown in Fig. 4b. When the tempera-

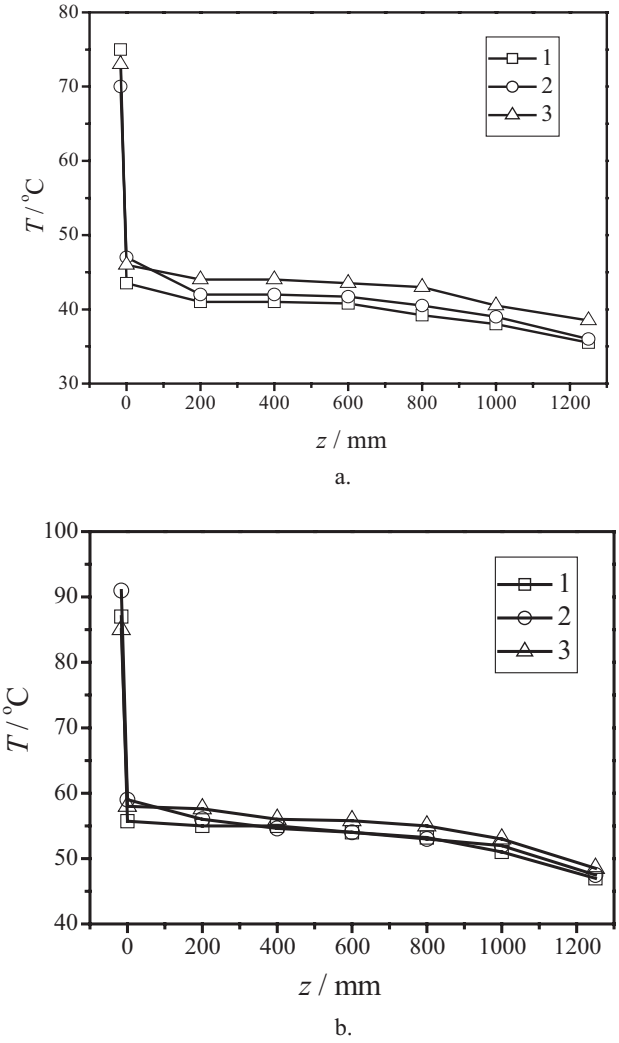

Figure 4. Temperature distributions of the tower in stable granulation processes; a. 58# wax; b. 70# wax.

ture in the granulation hole is above 75 °C, and the temperature in the tower is in the range 50–55 °C, stable granulation can be performed.

4.2.2 Particle Movement in the Tower

The spherical drops rise in the granulation hole and in the tower. After acceleration for a short time, the drop reaches its terminal velocity, at which the buoyancy F_B and the drag force F_D are balanced.

$$F_B - F_D = 0 \tag{10}$$

where

$$F_B = \frac{1}{6}\pi d_p^3 \rho_c g - \frac{1}{6}\pi d_p^3 \rho_d g \tag{11}$$

$$F_D = C_D A_p \frac{\rho_c u_t^2}{2} \tag{12}$$

where A_p is the projected particle area in direction of motion, equal to $\frac{\pi}{4}d_p^2$, cm^2; u_t is the terminal velocity, cm/s; d_p is the diameter of the particle, cm; C_D is the drag coefficient. The particle terminal velocity can be calculated from Eq. (10)–(12).

Calculation results show that the rising velocities of 4–5 mm particles are 130–150 mm/s for 58# semi-refined wax and 140–170 mm/s for 70# crystallitic wax, respectively. Combining with the minimum cooling times, which are given above, the suitable heights of the cooling tower for granulation of 58# semi-refined wax and 70# crystallitic wax are 910–1200 mm and 840–1190 mm, respectively.

Based on the calculated results, the height of the cooling tower is taken as 1250 mm and the residence time of the particle in the tower is about 8 seconds. Experimental results show that the cooling tower of 1250 mm height can ensure stable granulation.

4.3 Dehydration of Wax Particles

After the secondary stage cooling by water spraying, the wax particles are sent to a vibratory screen. Dehydration on the screen reduces the free water content on the particle surface to below 2 % for particles of 4–5 mm diameter. Due to the strong hydrophobicity of the wax, free water on the particle surface can easily be removed in a fluidized bed with heated air. Experiments show that free water on the particle surface is completely removed in the fluidized bed. The temperature of the fluidizing air needs to be experimentally determined. When the temperature is too high, the particles tend to be sticky and are difficult to fluidize. When the temperature is too low, it needs longer drying time to remove the free water and abrasion in the particles increases. Suitable conditions for 58# semi-refined wax and 70# crystallitic wax particles dehydration are 40 °C fluidizing air of 30 % relative humidity and 5 minutes residence time.

5 Granulation Results

The melted 58# semi-refined wax and 70# crystallitic wax are used as the feeds for granulation in the experiments. Using 118 nozzles (nozzle B), stable granulation is performed at a capacity of 55–60 kg/h. The sample images of the granulated particles are shown in Fig. 5. Fig. 5a and b show 4–5 mm particle samples of 58# semi-refined wax and 70# crystallitic wax, respectively. The corresponding nozzle inner and outer diameters are 0.97 mm and 1.28 mm, respectively. These figures show that the particles have good sphericity and a uniform size distribution. Some slight trailing vortices form during the rising of the wax drops in the tower, which are more obvious in large particles than in small particles. However, the trailing vortices do not influence the quality of the wax.

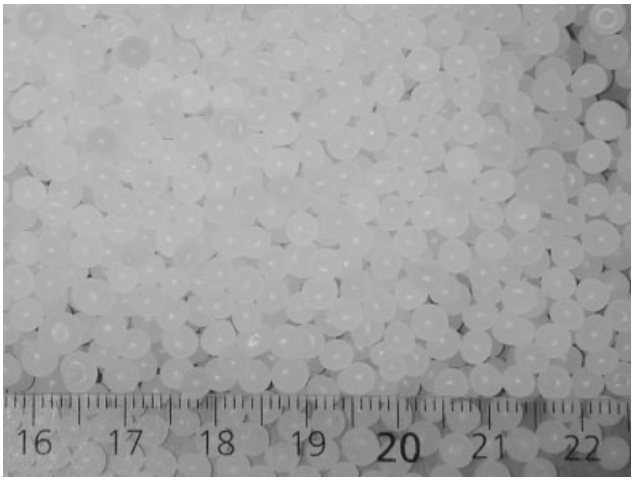

a.

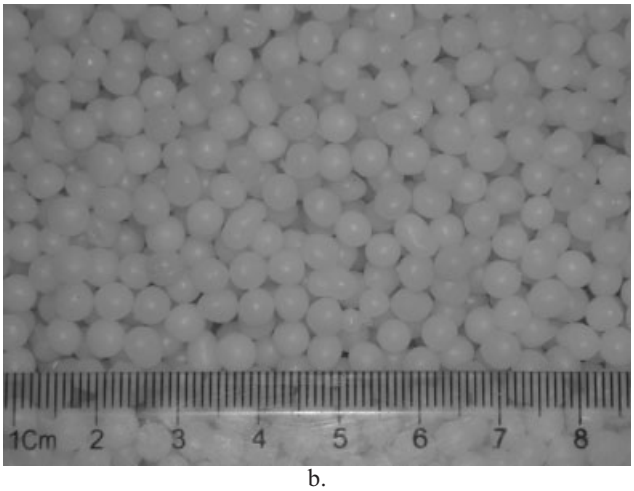

b.

Figure 5. Wax particles obtained in experiments; a. 58#, d_p = 4–5 mm; b. 70#, d_p = 4–5 mm.

6 Prediction of the Granulation Process

6.1 Prediction of the Particle Size

The granulation process includes wax drop formation, cooling of the drop and dehydration of the particles. The size of the wax particle is determined by the size of the drop formed in the granulation hole. The particle size can be predicted by conversion of the calculated drop size according to their density difference.

In calculating the drop size, the correlation of Scheele and Meister [4] is a suitable model. When it was used to calculate the drop volume for liquid systems of low viscosity and the inner diameter of the nozzle was within 0.0813–0.688 cm, the average error of correlation was 11 %. However, the model of Scheele and Meister did not take into account the wetting effect of the drop liquid with the nozzle. Therefore, when the dispersed phase preferentially wets the nozzle, the correlation of Scheele and Meister usually underestimates the drop size as much as 55 % [9].

Godfrey *et al.* [10] indicated that the liquid velocity through the nozzle and the wetting characteristics of the liquid with the nozzle tip are two important factors affecting drop formation. The investigations of Haynes *et al.* [11] and Hozawa *et al.* [12] showed that wettability and the Liquid-liquid-solid contact line significantly affect the drop formation from a nozzle with a flat tip. It was found that the wall thickness of the nozzle affects the size and size distribution of the drops [13,14]. Buchanan [15] reported that if the velocity of the dispersed phase from the nozzle is not much higher than the jetting velocity, the influence on the drop size by the wettability of the drop liquid with the nozzle tip cannot be ignored.

As can be seen from the above references [9–15], when the dispersed phase wets the nozzle tip more preferentially than the continuous phase does, the inner diameter of the nozzle in the expression of the four forces cannot be used for calculating the drop volume. In this situation, a virtual diameter, namely a characteristic diameter, should be introduced into the calculation of the drop size. If the continuous phase wets the nozzle tip more preferentially than the dispersed phase does, the inner diameter of the nozzle in the above equations should be taken as the characteristic diameter, and otherwise, the outside diameter should be taken as the characteristic diameter [11].

For small nozzles with thin walls, the contact lines of the three phases may move to the outer circumference of the nozzle tip and extend to the outside wall when the dispersed phase preferentially wets the nozzle, consequently, forming a larger drop.

Chen *et al.* [9] took account of the wetting effect of the drop liquid with the tip of the nozzle. It was pointed out that the outside diameter of the nozzle can be used as the characteristic diameter for large nozzles with thick walls (outside diameter around 10 mm and wall thickness range from 0.98 to 1.7 mm), and 1.15 times the outside diameter of the nozzle can be used as the characteristic diameter for small nozzles with thin walls (outside diameter less than 3.5 mm, and wall thickness less than 0.36 mm). For small nozzles with thin walls, Chen *et al.* indicated that when the characteristic diameter of $D_N = 1.15\ D_o$ was used, the agreement between experimentally measured sizes of the drops and the calculated values from Scheele and Meister's equations was reasonably good. The average error when using D_o and $1.15\ D_o$ as characteristic diameters was 11.42 % to 1.1 %, respectively.

Compared with the continuous phase of the water, the 58# semi-refined wax used in the experiments preferentially wets the nozzle and the geometries of the nozzle used are in the category of small nozzles with thin walls (the outside diameter is less than 3.5 mm, and the wall thickness is less than 0.36 mm). Therefore, the characteristic diameter of $D_N = 1.15\ D_o$ is used to calculate the wax drop volume.

Table 2. Dimensions of the nozzles.

Nozzle	A	B	C	D
D_i, mm	0.47	0.96	1.32	1.48
D_o, mm	0.80	1.28	1.64	1.83

The geometries of the stainless nozzles are listed in Tab. 2. Since the viscosity of water is lower than 10 centipoises, the drag term is negligible in the equations. With the temperatures of melted wax and water at 70 °C, the drop diameters are calculated by using the modified correlation of Scheele and Meister. Then, the solid particle diameters are acquired by conversion of the drop diameters according to their density difference. Wax particle diameters are plotted against volumetric flow rate in Fig. 6. As can be seen from Fig. 6 the particle diameter increases initially with volumetric flow rate, reaches a maximum and then gradually decreases. This behavior could be attributed to the change of the inertial force and the volume increase of the drop during the second stage.

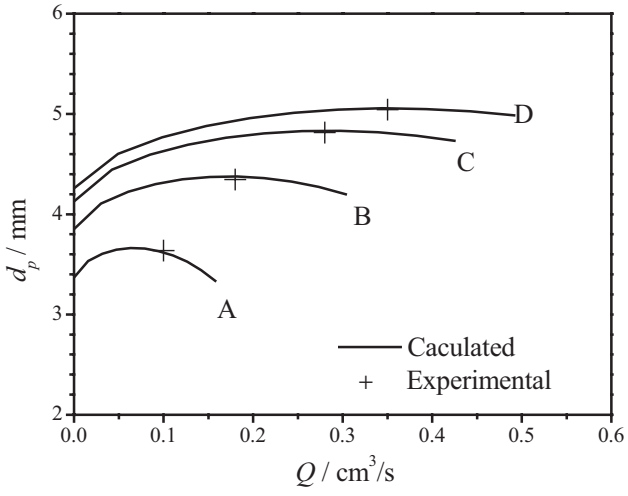

Figure 6. Particle diameter vs. volumetric flow rate for nozzles A, B, C, D and average particle diameters in experiments (58# semi-refined wax).

What needs to be indicated is that the effect of wall, the buoyancy lift, which resulted from upward water flow (caused by water temperature difference), and the disturbance of water in the hole are not considered in the calculation due to the complexity of conditions, which may result in error in prediction.

To evaluate the accuracy of the calculated results, the calculated results are compared with the experimental data. The experimental data for nozzles A, C, and D are acquired from a smaller experimental apparatus. The average diameters of the wax particles obtained in experiments are shown in Fig. 6. The calculated diameter of the wax particles are consistent with the experimental results, which show that the modified correlation of Scheele and Meister is of reasonable accuracy in predicting the volume or diameter of the wax particle. The modified correlation of Scheele and Meister, therefore, can be used to predict suitable operation flow rates and the corresponding particle diameters for different nozzles.

6.2 Operation Regime

When melted wax is injected into immiscible water through nozzles at a relatively low velocity, drops form directly at the nozzle tip and break off when the wax drop reaches a certain size. When the velocity of the melted wax through the nozzle is higher than the critical velocity, called the jetting velocity, a jet forms. The jet then breaks into small drops. These small drops easily cause jam of the granulation hole and agglomerate in the tower, which results in an unstable granulation. Therefore, the operating velocity of the melted wax flow in the nozzle should be lower than the jetting velocity.

Scheele and Meister [4] considered that a jet results when sufficient upward forces at the nozzle exit. The upward forces consist of the force F_P and the inertial force F_I. To form a jet, the net upward force at the nozzle tip must overcome the interfacial tension force. The critical jetting velocity is given:

$$u_J = 1.73\left[\frac{\sigma}{\rho_d D_N}\left(1-\frac{D_N}{D_E}\right)\right]^{1/2} \tag{13}$$

To ensure stability of wax granulation and to increase the production capacity for each single nozzle, the volumetric flow rate should be in a suitable range. The operation regime of the volumetric flow rate is taken to be 0.6~0.85 times of the critical jetting flow rate. Consequently, under given experimental conditions, the suitable range of the volumetric flow rate can be calculated. For 58# semi-refined wax, the suitable operation regime of the volumetric flow rate and the range of the corresponding diameters of the wax particles for different nozzles are listed in Tab. 3. For a required diameter of the product, the suitable nozzle and the range of volumetric flow rate can be determined from Tab. 3. For 70# crystallitic wax, the calculated results and experimental data for nozzle B are listed in Tab. 4.

Fig. 7 shows that the nozzle volumetric flow rate increase with the nozzle diameter at critical state. It is of significance for practical applications to predict the nozzle volumetric flow rate at critical state for different nozzle diameters.

Table 3. Prediction of the suitable operation flow rates and the corresponding particle diameters for 58# semi-refined wax.

Nozzle	A	B	C	D
Volumetric flow rate, cm^3/s	0.09–0.13	0.18–0.26	0.25–0.36	0.29–0.42
Diameter of the particle, mm	3.48–3.63	4.30–4.37	4.80–4.83	5.04–5.06

Table 4. Calculated and experimental flow rates and the corresponding particle diameters for 70# crystallitic wax with nozzle B.

Wax	70# crystallitic wax	
Calculated	Volumetric flow rate, cm^3/s	0.18–0.25
	Diameter of the particle, mm	4.28–4.47
Experimental	Average volumetric flow rate, cm^3/s.	0.21
	Average particle diameter, mm	4.45

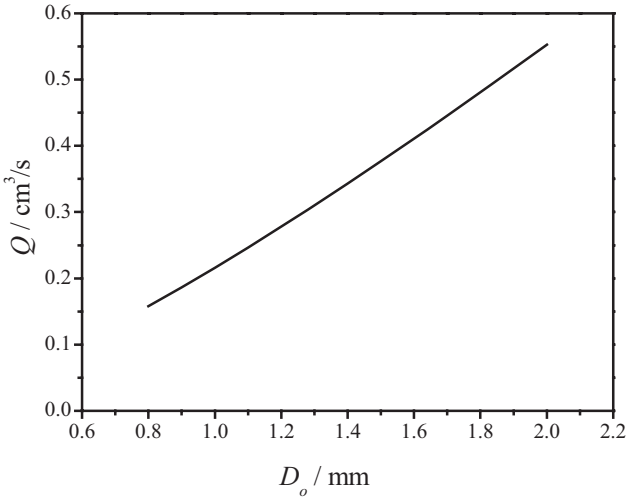

Figure 7. Nozzle volumetric flow rate vs. nozzle outside diameter at the critical state.

7 Conclusions

A novel granulation technology for producing spherical wax particles by using the insolubility of wax and water is developed. The granulation with melted 58# semi-refined wax and 70# crystallitic wax is stably preformed in an experimental granulator with 118 nozzles (D_i = 0.96, D_o = 1.28) at a capacity of 55–60 kg/h. Spherical wax particles with a uniform diameter are obtained. The suitable operation parameters are obtained from calculation and experiments.

In the novel technology, two special components, namely the switch board controlled by temperature and the heating board with granulation holes are designed and used. By controlling the temperature of the switch board, the switching function is performed flexible. The granulation hole in the heating board ensures stable granulation and reduced energy consumption.

Using the modified correlation of Scheele and Meister, suitable operation flow rates and the corresponding particle diameters for different nozzles are predicted. The comparison between the calculated results and the experimental data shows that the prediction is of reasonable accuracy.

The granulation process has large process capacity and high heat-transfer efficiency while using a small space for the granulator. It is easy to scaleup by increasing more granulation elements in one granulator. The granulation process can be used to produce particles of different brands of wax, and also to produce particles of other materials which have similar physical properties, such as sulphur, rosin, alum and some age-inhibiting agents of rubbers, etc. For specific materials, the corresponding granulator structure may need to be re-designed.

Acknowledgment

The authors wish to express their appreciation for the financial support of this study by China National Petroleum Corporation (CNPC) Innovation Fund. The grant number is No. 03E7039.

Received: January 30, 2004 [CET 2036]

Symbols used

A_p	[cm^2]	projected particle area in direction of motion
C_D	[–]	drag coefficient
D_E	[cm]	diameter of detached drop
D_i	[cm]	inner diameter of the nozzle
D_N	[cm]	characteristic diameter of the nozzle
D_o	[cm]	outer diameter of the nozzle
d_p	[cm]	diameter of the particle
F	[–]	Harkins and Brown's correction factor
F_B	[dynes]	buoyancy force
F_D	[dynes]	drag force
F_I	[dynes]	inertial force
F_P	[dynes]	excess pressure force
F_S	[dynes]	interfacial tension force
t	[s]	time
T_l	[°C]	temperature of liquid phase
T_s	[°C]	temperature of solid phase
Q	[cm^3/s]	volumetric flow rate of dispersed phase
u_J	[cm/s]	critical jetting velocity at which a jet first forms
u_N	[cm/s]	average velocity of the dispersed phase through the nozzle
u_t	[cm/s]	terminal velocity
V_E	[cm^3]	drop volume after break off from the nozzle
V_{EN}	[cm^3]	volumetric flow out of the nozzle during the second stage
V_{ES}	[cm^3]	drop volume at the end of the first stage

Greek symbols

α_l	[m^2/s]	thermal diffusivity of liquid phase
α_s	[m^2/s]	thermal diffusivity of solid phase
κ_l	[W/(m·K)]	thermal conductivity of liquid phase
κ_s	[W/(m·K)]	thermal conductivity of solid phase
λ	[J/kg]	latent heat of phase change
μ_c	[g/(cm·s)]	viscosity of continuous phase
μ_d	[g/(cm·s)]	viscosity of dispersed phase
v_ξ	[m/s]	moving velocity of the solid-liquid interface
ξ	[–]	solid-liquid interface
ρ_c	[g/cm^3]	density of continuous phase
ρ_d	[g/cm^3]	density of dispersed phase
$\Delta\rho$	[g/cm^3]	density difference
σ	[dyne/cm]	interfacial tension

References

[1] P. Y. Chu, *Liaoning Chemical Industry* **1998**, *27(3)*, 139.
[2] X. Y. Fan, *Petrochemical Industry Trends* **1999**, *7(2),* 33.
[3] E. V. L. Narasinga Rao, R. Kumar, N. R. Kuloor, *Chem. Eng. Sci.* **1966**, *21*, 867.
[4] G. F. Scheele, B. J. Meister, *AIChE J.* **1968**, *14(1)*, 9.
[5] W. D. Harkins, F. E. Brown, *J. Am. Chem. Soc.* **1919**, *4*, 499.
[6] M. Horvath, L. Steiner, S. Hartland, *Can. J. Chem. Eng.* **1978**, *56*, 9.
[7] R. I. Pedrose, G. A. Domoto, *Int. J. Heat Mass Transfer* **1974**, *17*, 1507.
[8] C. Kim, M. Kaviany, *Int. J. Heat Mass Transfer* **1990**, *33(12)*, 2721.
[9] C. T. Chen, J. R. Maa, Y. M. Yang, C. H. Chang *et. al.*, *Int. Comm. Heat Mass Transfer* **2001**, *28(5)*, 681.
[10] J. C. Godfrey, C. Hanson, Liquid-Liquid Systems, in *Handbook of Multiphase Systems*, (Ed: G. Hetsroni), Hemisphere, Washington **1982**, 1–46.
[11] L. G. Haynes, D. M. Himmelblau, R. S. Schechter, *Ind. Eng. Chem. Process Des. Dev.* **1968**, *7(4)*, 508.
[12] M. Hozawa, T. Tsukada, N. Imaishi, K. Fjuinawa, *J. Chem. Eng. Japan* **1981**, *14(5)*, 358.
[13] A. Eckstein, A. Vogelpohl, *Chem. Eng. Technol. Part A* **1998**, *21(12)*, 952.
[14] A. Eckstein, A. Vogelpohl, *Chem. Eng. Technol. Part A* **1999**, *22(1)*, 23.
[15] R. H. Buchana, *Australian J. Appl. Sci.* **1952**, *3*, 233.

